Progress In Electromagnetics Research, PIER 73, 71–91, 2007

ELECTROMAGNETIC FIELD FROM A HORIZONTAL ELECTRIC DIPOLE ON THE SURFACE OF A HIGH LOSSY DIELECTRIC COATED WITH A UNIAXIAL LAYER

J. P. Mei and K. Li

The Electromagnetics Academy
Zhejiang University
Hangzhou 310058, China

Abstract—In this paper, the explicit formulas are derived for the six components of the electromagnetic field in air excited by a horizontal electric dipole over a planar high lossy dielectric coated with an anisotropic uniaxial layer. Similar to the case of the three-layered region consisting of air, a uniaxial layer, and a perfect conductor, the total field consists of the direct field, the ideal reflected field or the field of an ideal image, the lateral-wave field, and the trapped-surface-wave field. It should be pointed out that the trapped surface wave can be separated into the trapped wave of electric type and magnetic type. The wave numbers in the $\hat{\rho}$ direction of electric-type trapped surface wave, which are between k_0 and k_L, are different from those of the magnetic-type trapped surface wave, which are between k_0 and k_T. When the thickness l of the uniaxial layer satisfies $n\pi < \frac{k_T}{k_L}(k_L^2 - k_0^2)^{1/2} \cdot l < (n+1)\pi$, there are $n+1$ modes of the electric-type trapped surface waves. When the thickness l satisfies $(n-\frac{1}{2})\pi < (k_T^2 - k_0^2)^{1/2} \cdot l < (n+\frac{1}{2})\pi$, there are n modes of magnetic-type trapped waves.

1. INTRODUCTION

The electromagnetic fields generated by horizontal and vertical electric dipoles in a three-layered planar region have been visited by many investigators [1–10]. In early 1990s, King *et al.* had presented the simple analytical formulas for the electromagnetic fields of horizontal and vertical electric dipoles in the presence of the three-layered planar region [2–4]. In 1998, Wait [5] presented a comment on [4] and claimed

that King and Sandle had overlooked the trapped-surface-wave term, which varies as $\rho^{-1/2}$ in the far region. To clarify the debate, the old problem had been re-visited in several papers [7–9]. It has been concluded that the trapped surface wave can be excited efficiently by horizontal and vertical dipoles in three-layered region.

Recently, Li and Lu [10] have visited the electromagnetic field excited by a horizontal electric dipole in a three-layered planar region consisting of a perfect conductor coated with a uniaxially anisotropic layer under the air. In many actual cases, the layer under the uniaxial layer is a lossy medium. In what follows, with the extension of [10], the similar derivations and computations will be carried out for the electromagnetic field in air excited by a horizontal electric dipole over a planar high lossy dielectric coated with an anisotropic uniaxial layer.

2. ELECTROMAGNETIC FIELD IN AIR OF A HORIZONTAL ELECTRIC DIPOLE ON A LOSSY MEDIUM COATED WITH A UNIAXIALLY ANISOTROPIC LAYER

2.1. Integrated Representations for the EM Field in Air of a Horizonal Dipole

In this section, the integrated formulas are derived for six components of the electromagnetic field in the air due to a horizonal electric dipole for the three-layered planar region consisting of a lossy dielectric coated with an uniaxially anisotropic layer under the air. The relevant

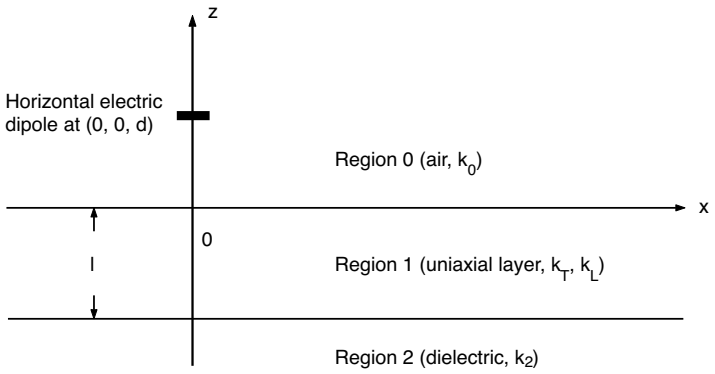

Figure 1. Geometry of a $\hat{x}$-directed horizontal electric dipole on or close to the surface of a dielectric coated with a uniaxially anisotropic layer.

geometry and Cartesian coordinate system are illustrated in Fig. 1, where a unit horizontal electric dipole in the $\hat{x}$ direction is located at $(0, 0, d)$. Region 0 ($z \geq 0$) is the upper space above the uniaxial layer occupied with the air, Region 1 ($-l \leq z \leq 0$) is the anisotropic uniaxial layer characterized by a permittivity tensor of the form

$$\hat{\varepsilon}_1 = \varepsilon_0 \begin{bmatrix} \varepsilon_T & 0 & 0 \\ 0 & \varepsilon_T & 0 \\ 0 & 0 & \varepsilon_L \end{bmatrix}. \tag{1}$$

and Region 2 ($z \leq -l$) is occupied by the lossy dielectric. It is assumed that Regions 0, 1, and 2 are nonmagnetic so that $\mu_0 = \mu_1 = \mu_2$. So that the wave numbers of the three regions are

$$\begin{aligned} k_0 &= \omega\sqrt{\mu_0\varepsilon_0} \\ k_T &= \omega\sqrt{\mu_0\varepsilon_0\varepsilon_T}, \qquad k_L = \omega\sqrt{\mu_0\varepsilon_0\varepsilon_L} \\ k_2 &= \omega\sqrt{\mu_0\varepsilon_0\hat{\varepsilon}_2} \end{aligned} \tag{2}$$

where $\hat{\varepsilon}_2 = \varepsilon_2 - i\frac{\sigma_2}{\varepsilon_0\omega}$, ε_2 is the relative permittivity of Region 2, and σ_2 is the conductivity of Region 2. With the time dependence $e^{-i\omega t}$, Maxwell's equations in the three regions can be expressed by

$$\nabla \times \mathbf{E}_j = i\omega\mathbf{B}_j \tag{3}$$

$$\nabla \times \mathbf{B}_j = \mu_0\left(-i\omega\hat{\varepsilon}_j\mathbf{E}_j + \hat{x}J_x^e\right) \tag{4}$$

where

$$J_x^e = Idl\delta(x)\delta(y)\delta(z-d) \tag{5}$$

is the volume current density in the dipole.

On the interface at $z = 0$ between Region 0 and Region 1, the fields should satisfy the following boundary conditions

$$E_{1x}(x, y, 0) = E_{0x}(x, y, 0) \tag{6}$$

$$E_{1y}(x, y, 0) = E_{0y}(x, y, 0) \tag{7}$$

$$k_L E_{1z}(x, y, 0) = k_0 E_{0z}(x, y, 0) \tag{8}$$

$$\mathbf{B}_1(x, y, 0) = \mathbf{B}_0(x, y, 0). \tag{9}$$

Similarly, on the interface at $z = -l$ between Region 1 and Region 2 should satisfy the following boundary conditions

$$E_{2x}(x, y, -l) = E_{1x}(x, y, -l) \tag{10}$$

$$E_{2y}(x, y, -l) = E_{1y}(x, y, -l) \tag{11}$$

$$k_2 E_{2z}(x, y, -l) = k_L E_{1z}(x, y, -l) \tag{12}$$

$$\mathbf{B}_2(x, y, -l) = \mathbf{B}_1(x, y, -l). \tag{13}$$

With the extension of [10], the formulas are derived readily for the six components of the electromagnetic field in air due to a horizonal electric dipole. They are

$$\begin{aligned} E_{0\rho}(\rho,\varphi,z) &= -\frac{\omega\mu_0 Idl}{4\pi k_0^2}\cdot\cos\varphi \\ &\quad\cdot[F_{\rho 0}(\rho,z-d)-F_{\rho 0}(\rho,z+d)+F_{\rho 1}(\rho,z+d)] \qquad (14) \\ E_{0\varphi}(\rho,\varphi,z) &= \frac{\omega\mu_0 Idl}{4\pi k_0^2}\cdot\sin\varphi \\ &\quad\cdot[F_{\varphi 0}(\rho,z-d)-F_{\varphi 0}(\rho,z+d)+F_{\varphi 1}(\rho,z+d)] \qquad (15) \\ E_{0z}(\rho,\varphi,z) &= \frac{i\omega\mu_0 Idl}{4\pi k_0^2}\cdot\cos\varphi \\ &\quad\cdot[F_{z0}(\rho,z-d)-F_{z0}(\rho,z+d)+F_{z1}(\rho,z+d)] \qquad (16) \\ B_{0\rho}(\rho,\varphi,z) &= -\frac{\mu_0 Idl}{4\pi}\cdot\sin\varphi \\ &\quad\cdot[G_{\rho 0}(\rho,z-d)-G_{\rho 0}(\rho,z+d)+G_{\rho 1}(\rho,z+d)] \qquad (17) \\ B_{0\varphi}(\rho,\varphi,z) &= -\frac{\mu_0 Idl}{4\pi}\cdot\cos\varphi \\ &\quad\cdot[G_{\varphi 0}(\rho,z-d)-G_{\varphi 0}(\rho,z+d)+G_{\varphi 1}(\rho,z+d)] \qquad (18) \\ B_{0z}(\rho,\varphi,z) &= \frac{i\mu_0 Idl}{4\pi}\cdot\sin\varphi \\ &\quad\cdot[G_{z0}(\rho,z-d)-G_{z0}(\rho,z+d)+G_{z1}(\rho,z+d)]. \qquad (19) \end{aligned}$$

In order to contrast with the available results, the formulas of the above six components for the uniaxially anisotropic case are written in the similar forms as addressed in [2, 9, 10]. In these formulas, $F_{m0}(\rho,z-d)$ and $G_{m0}(\rho,z-d)$ ($m=\rho,\varphi$ and z) represent the direct field of the horizontal dipole at $(0,0,d)$, and $F_{m0}(\rho,z+d)$ and $G_{m0}(\rho,z+d)$ represent the ideal reflected field or the field of a ideal image dipole at $(0,0,-d)$. It is noted that the integrals for the direct and ideally reflected fields in the air of the horizontal dipole over perfect conductor or a lossy dielectric coated with the isotropic or anisotropic layer are same. The values $F_{m0}(\rho,z\pm d)$ and $G_{m0}(\rho,z\pm d)$ ($m=\rho,\varphi$ and z) had been evaluated by King in [2, 3], and will not be duplicated in this paper.

Next, emphasis is placed on finding a solution of the last terms in the brackets in (14)–(19) by using analytical techniques. The last terms are expressed as the same forms in [2, 9], and [10]. They are

$$\begin{aligned} F_{\rho 1}(\rho,z+d) &= F_{\rho 2}(\rho,z+d)+F_{\rho 3}(\rho,z+d) \qquad (20) \\ F_{\varphi 1}(\rho,z+d) &= F_{\varphi 2}(\rho,z+d)+F_{\varphi 3}(\rho,z+d) \qquad (21) \end{aligned}$$

$$G_{\rho 1}(\rho, z+d) = G_{\rho 2}(\rho, z+d) + G_{\rho 3}(\rho, z+d) \quad (22)$$

$$G_{\varphi 1}(\rho, z+d) = G_{\varphi 2}(\rho, z+d) + G_{\varphi 3}(\rho, z+d) \quad (23)$$

where

$$\begin{matrix} F_{\rho 2}(\rho, z+d) \\ F_{\varphi 2}(\rho, z+d) \end{matrix} = \frac{1}{2}\int_0^\infty \gamma_0(Q_3+1)[J_0(\lambda\rho) \mp J_2(\lambda\rho)] \cdot e^{i\gamma_0(z+d)}\lambda d\lambda \quad (24)$$

$$\begin{matrix} F_{\rho 3}(\rho, z+d) \\ F_{\varphi 3}(\rho, z+d) \end{matrix} = -\frac{k_0^2}{2}\int_0^\infty \gamma_0^{-1}(P_3-1)[J_0(\lambda\rho) \pm J_2(\lambda\rho)] \cdot e^{i\gamma_0(z+d)}\lambda d\lambda \quad (25)$$

$$\begin{matrix} G_{\rho 2}(\rho, z+d) \\ G_{\varphi 2}(\rho, z+d) \end{matrix} = \frac{1}{2}\int_0^\infty (Q_3+1)\left[J_0(\lambda\rho) \pm J_2(\lambda\rho)\right] \cdot e^{i\gamma_0(z+d)}\lambda d\lambda \quad (26)$$

$$\begin{matrix} G_{\rho 3}(\rho, z+d) \\ G_{\varphi 3}(\rho, z+d) \end{matrix} = -\frac{1}{2}\int_0^\infty (P_3-1)\left[J_0(\lambda\rho) \mp J_2(\lambda\rho)\right] \cdot e^{i\gamma_0(z+d)}\lambda d\lambda \quad (27)$$

$$F_{z1}(\rho, z+d) = \int_0^\infty (Q_3+1)J_1(\lambda\rho)e^{i\gamma_0(z+d)}\lambda^2 d\lambda \quad (28)$$

$$G_{z1}(\rho, z+d) = -\int_0^\infty \gamma_0^{-1}(P_3-1)J_1(\lambda\rho)e^{i\gamma_0(z+d)}\lambda^2 d\lambda. \quad (29)$$

The integrals F_{z1}, $F_{\rho 2}$, $F_{\varphi 2}$, $G_{\rho 2}$, and $G_{\varphi 2}$ involving (Q_3+1) are defined as the terms of the electric-type (TM mode) field. The integrals G_{z1}, $F_{\rho 3}$, $F_{\varphi 3}$, $G_{\rho 3}$, and $G_{\varphi 3}$ involving (P_3-1) are defined as the terms of the magnetic-type (TE mode) field. The factors (Q_3+1) and (P_3-1) are expressed as

$$\begin{aligned} \frac{\gamma_0}{2}(Q_3+1) &= \gamma_0\left(\frac{\gamma_2}{k_2^2} - \frac{i\gamma_L \tan\gamma_L l}{k_T^2}\right) \\ &\quad \cdot\left[\frac{\gamma_0}{k_0^2} + \frac{\gamma_2}{k_2^2} - i\left(\frac{\gamma_L}{k_T^2} + \frac{k_T^2\gamma_0\gamma_2}{k_0^2 k_2^2\gamma_L}\right)\cdot\tan\gamma_L l\right]^{-1} \quad (30) \\ \frac{k_0^2}{2\gamma_0}(P_3-1) &= -k_0^2\left(\frac{\gamma_T}{\gamma_2} - i\tan\gamma_T l\right) \\ &\quad \cdot\left[\gamma_T + \frac{\gamma_T}{\gamma_2}\gamma_0 - i\left(\gamma_0 + \frac{\gamma_T^2}{\gamma_2}\right)\cdot\tan\gamma_T l\right]^{-1} \quad (31) \end{aligned}$$

where

$$\begin{aligned} \gamma_T^2 &= k_T^2 - \lambda^2, \qquad \mathrm{Im}\{\gamma_T\} > 0 \\ \gamma_L^2 &= \frac{{k_T}^2}{{k_L}^2}\left(k_L^2 - \lambda^2\right), \qquad \mathrm{Im}\{\gamma_L\} > 0 \\ \gamma_0^2 &= k_0^2 - \lambda^2, \qquad \mathrm{Im}\{\gamma_0\} > 0 \\ \gamma_2^2 &= k_2^2 - \lambda^2, \qquad \mathrm{Im}\{\gamma_2\} > 0 \end{aligned}$$

$$\begin{aligned}
\lambda^2 &= k_x^2 + k_y^2 \\
k_T^2 &= k_0^2\varepsilon_T, \qquad k_L^2 = k_0^2\varepsilon_L, \qquad k_2^2 = k_0^2\hat{\varepsilon}_2 \\
k_0 &= \omega\sqrt{\mu_0\varepsilon_0} = 2\pi/\lambda_0, \qquad \omega = 2\pi f.
\end{aligned} \tag{32}$$

Here f is the operating frequency and λ_0 is the wavelength in air.

2.2. Evaluation for the Terms of the Electric-type (TM) Field

All integrands in (26)–(29) converge very slowly for including Bessel functions $J_j(\lambda\rho)$ $(j = 0, 1, 2)$ with highly oscillatory. In what follows, we will attempt to evaluate these integrals by using analytical techniques. Considering γ_0, γ_T, and γ_L are even functions of λ, use is made of the following relations between Bessel function and Hankel function

$$J_n(\lambda\rho) = \frac{1}{2}\left[H_n^{(1)}(\lambda\rho) + H_n^{(2)}(\lambda\rho)\right] \tag{33}$$

$$H_n^{(1)}(-\lambda\rho) = (-1)^{n+1}H_n^{(2)}(\lambda\rho). \tag{34}$$

Substitution (33) and (34) into (24) yields to

$$\begin{aligned}
\begin{matrix} F_{\rho_2} \\ F_{\varphi_2} \end{matrix} = \frac{1}{2}\int_{-\infty}^{\infty} & \frac{\gamma_0\left(\dfrac{\gamma_2}{k_2^2} - \dfrac{i\gamma_L}{k_T^2}\tan\gamma_L l\right)e^{i\gamma_0(z+d)}}{\dfrac{\gamma_0}{k_0^2} + \dfrac{\gamma_2}{k_2^2} - i\left(\dfrac{\gamma_L}{k_T^2} + \dfrac{k_T^2\gamma_0\gamma_2}{k_0^2k_2^2\gamma_L}\right)\tan\gamma_L l} \\
& \cdot\left[H_0^{(1)}(\lambda\rho) \mp H_2^{(1)}(\lambda\rho)\right]\lambda d\lambda.
\end{aligned} \tag{35}$$

Following the similar method addressed in [8], the integrals in (35) can be evaluated readily. It is necessary to shift the contour around the branch lines at $\lambda = k_0$, $\lambda = k_L$, and $\lambda = k_2$ for evaluating the integral in (35). The configuration of the poles and the branch cuts are shown in Fig. 2. The poles of the integrands satisfy the following equation.

$$q(\lambda) = \frac{\gamma_0}{k_0^2} + \frac{\gamma_2}{k_2^2} - i\left(\frac{\gamma_L}{k_T^2} + \frac{k_T^2\gamma_0\gamma_2}{k_0^2k_2^2\gamma_L}\right)\tan\gamma_L l = 0. \tag{36}$$

When $k_2 \to \infty$, the above pole equation reduces to (29) in [10]. In order to analyze the pole equation, it is necessary to define a value $s = k_0/k_2$, which a perfect conductor or dielectric can be characterized. For the perfect conductor case, $k_2 \to \infty$, s=0. For the dielectric case, s will be a complex number with its magnitude being less than 1 and its

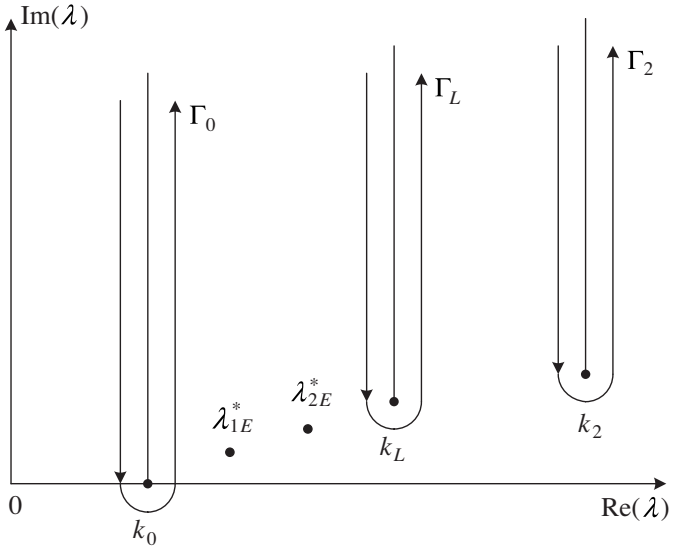

Figure 2. The configuration of the poles and the branch cuts for the electric-type (TM) field.

phase being from 0° to 45°. Then the pole equation can be rewritten as follows:

$$q(s,\lambda) = \frac{\gamma_0}{k_0^2} + \frac{s\sqrt{1-s^2\lambda^2/k_0^2}}{k_0} - i\left(\frac{\gamma_0 s\sqrt{1-s^2\lambda^2/k_0^2}k_T^2}{\gamma_L k_0^3} + \frac{\gamma_L}{k_T^2}\right)\tan(\gamma_L l) = 0. \tag{37}$$

Assuming that λ_{jE}^* is the j-th root of (37), we have

$$\gamma_{0E}^* = \sqrt{k_0^2 - \lambda_{jE}^{*2}} \tag{38}$$

$$\gamma_L^* = \frac{k_T}{k_L}\sqrt{k_L^2 - \lambda_{jE}^{*2}} \tag{39}$$

$$\gamma_{2E}^* = \sqrt{k_2^2 - \lambda_{jE}^{*2}}. \tag{40}$$

It is seen that F_{ρ_2} and F_{φ_2} can be re-written as in the following forms.

$$\begin{matrix} F_{\rho_2} \\ F_{\varphi_2} \end{matrix} = i\pi \sum_j \frac{\gamma_{0E}^*\left(\dfrac{\gamma_{2E}^*}{k_2^2} - \dfrac{i\gamma_L^*}{k_T^2}\tan\gamma_L^* l\right)}{q'(\lambda_{jE}^*)} e^{i\gamma_{0E}^*(z+d)}\lambda_{jE}^*$$

$$\cdot \left[H_0^{(1)}(\lambda_{jE}^*\rho) \mp H_2^{(1)}(\lambda_{jE}^*\rho)\right]$$
$$+\frac{1}{2}\int_{\Gamma_0+\Gamma_L+\Gamma_2} \frac{\gamma_0\left(\frac{\gamma_2}{k_2^2} - \frac{i\gamma_L}{k_T^2}\tan\gamma_L l\right)e^{i\gamma_0(z+d)}}{q(\lambda)}$$
$$\cdot \left[H_0^{(1)}(\lambda\rho) \mp H_2^{(1)}(\lambda\rho)\right]\cdot \lambda d\lambda \tag{41}$$

where

$$\begin{aligned} q'(\lambda_{jE}^*) \;=\; & -\frac{\lambda_{jE}^*}{k_0^2\gamma_0^*} - \frac{\lambda_{jE}^*}{k_2^2\gamma_2^*} \\ & -i\tan\gamma_L^* l\Big[-\frac{\lambda_{jE}^*}{k_T^2\gamma_L^*} + \frac{k_T^2}{k_0^2k_2^2}\Big(-\frac{\lambda_{jE}^*\gamma_2^*}{\gamma_0^*\gamma_L^*} - \frac{\lambda_{jE}^*\gamma_0^*}{\gamma_2^*\gamma_L^*} + \frac{\lambda_{jE}^*\gamma_0^*\gamma_2^*}{\gamma_L^{*3}}\Big)\Big] \\ & +i\sec^2\gamma_L^* l\Big(\frac{\gamma_L^*}{k_T^2} + \frac{k_T^2\gamma_0^*\gamma_2^*}{k_0^2k_2^2\gamma_L^*}\Big)\frac{\lambda_{jE}^* l}{\gamma_L^*}. \end{aligned} \tag{42}$$

In general, when the thickness of the uniaxially anisotropic layer satisfies $n\pi < \frac{k_T}{k_L}\sqrt{k_L^2 - k_0^2}l < (n+1)\pi$, Eq. (36) has $n+1$ roots. Correspondingly, the terms of the trapped surface wave have $n+1$ modes.

Next, it is necessary to evaluate the integrals along the branch lines Γ_0, Γ_L, and Γ_2. Following the similar procedures addressed in [7–10], three integrals in (41) can be evaluated readily. First, we will examine the branch cut Γ_L as shown in Fig. 2. Because the phase of the branch cut Γ_L remains the same value on both sides, it is seen that the evaluation of the integral along the branch line Γ_L is zero. With Region 2 being a high lossy medium, the integration along the branch cut Γ_2 can be neglected.

Considering the conditions $k_0\rho \gg 1$ and $z + d \ll \rho$, the dominant contribution of the integral in (41) along the branch line Γ_0 comes from the vicinity of k_0. The parameter $\lambda = k_0(1 + i\tau^2)$ is used for the integration. At the vicinity of k_0, γ_0, γ_L, and γ_2 are approximated as

$$\gamma_0 \;\approx\; \sqrt{2}k_0 e^{i\frac{3\pi}{4}}\tau \tag{43}$$
$$\gamma_L \;\approx\; \gamma_L' = \frac{k_T}{k_L}\sqrt{k_L^2 - k_0^2} \tag{44}$$
$$\gamma_2 \;\approx\; \gamma_2' = \sqrt{k_2^2 - k_0^2}. \tag{45}$$

Use is made of the following relations

$$e^{i\gamma_0(z+d)}\cdot e^{ik_0\rho-\frac{i\pi}{4}-k_0\rho\tau^2}=e^{ik_0\rho\left[1+\frac{1}{2}\left(\frac{z+d}{\rho}\right)^2\right]-\frac{i\pi}{4}}\cdot e^{-k_0\rho\left(\tau+\frac{e^{i\pi/4}}{\sqrt{2}}\frac{z+d}{\rho}\right)^2}. \tag{46}$$

Then, the integral along the branch cut Γ_0 in (41) can be written in the following form.

$$\begin{aligned}
I_1 &= \frac{1}{2}\int_{\Gamma_0}\frac{\gamma_0\left(\dfrac{\gamma_2}{k_2^2}-i\dfrac{\gamma_L}{k_T^2}\tan\gamma_L l\right)e^{i\gamma_0(z+d)}}{\dfrac{\gamma_0}{k_0^2}+\dfrac{\gamma_2}{k_2^2}-i\left(\dfrac{\gamma_L}{k_T^2}+\dfrac{k_T^2\gamma_0\gamma_2}{k_0^2k_2^2\gamma_L}\right)\tan\gamma_L l}\\
&\quad\cdot\left[H_0^{(1)}(\lambda\rho)\mp H_2^{(1)}(\lambda\rho)\right]\lambda d\lambda\\
&= 2e^{-i\frac{\pi}{4}}k_0^3A\sqrt{\frac{2}{\pi k_0\rho}}e^{ik_0r_2}\\
&\quad\cdot\Bigg\{-e^{i\frac{\pi}{4}}\sqrt{\frac{\pi}{2k_0\rho}}\left(\frac{z+d}{\rho}+iA\right)+\frac{\pi}{2}A^2\exp\left[-i\frac{k_0\rho}{2}\left(\frac{z+d}{\rho}-iA\right)^2\right]\\
&\quad\cdot erfc\left[\sqrt{-i\frac{k_0\rho}{2}\left(\frac{z+d}{\rho}-iA\right)^2}\right]\Bigg\}\cdot\begin{pmatrix}1\\-\frac{i}{k_0\rho}\end{pmatrix}
\end{aligned}\tag{47}$$

where

$$\begin{aligned}
A &= \frac{k_0\left(\dfrac{\gamma_L}{k_T^2}\tan\gamma_L l+i\dfrac{\gamma_2}{k_2^2}\right)}{1-i\dfrac{k_T^2\gamma_2}{k_2^2\gamma_L}\tan\gamma_L l}\\
&= \frac{k_0\left[\dfrac{\sqrt{k_L^2-k_0^2}}{k_Lk_T}\tan\left(\dfrac{k_T}{k_L}\sqrt{k_L^2-k_0^2}\cdot l\right)+i\dfrac{\sqrt{k_2^2-k_0^2}}{k_2^2}\right]}{1-i\dfrac{k_T^3k_L}{k_2^2}\dfrac{\sqrt{k_2^2-k_0^2}}{\sqrt{k_L^2-k_0^2}}\tan\left(\dfrac{k_T}{k_L}\sqrt{k_L^2-k_0^2}\cdot l\right)}.
\end{aligned}\tag{48}$$

Therefore the final expression of (35) can be obtained as follows:

$$\begin{matrix}F_{\rho_2}\\F_{\varphi_2}\end{matrix} = i\pi\sum_j\frac{\gamma_0^*\left(\dfrac{\gamma_2^*}{k_2^2}-\dfrac{i\gamma_L^*}{k_T^2}\tan\gamma_L^*l\right)}{q'\left(\lambda_{jE}^*\right)}e^{i\gamma_{0E}^*(z+d)}\lambda_{jE}^*$$

$$\cdot\left[H_0^{(1)}\left(\lambda_{jE}^*\rho\right) \mp H_2^{(1)}\left(\lambda_{jE}^*\rho\right)\right] + 2e^{-i\frac{\pi}{4}}k_0^3 A\sqrt{\frac{2}{\pi k_0\rho}}e^{ik_0r_2}$$
$$\cdot\left\{-e^{i\frac{\pi}{4}}\sqrt{\frac{\pi}{2k_0\rho}}\left(\frac{z+d}{\rho}+iA\right)+\frac{\pi}{2}A^2\exp\left[-i\frac{k_0\rho}{2}\left(\frac{z+d}{\rho}-iA\right)^2\right]\right.$$
$$\left.\cdot erfc\left[\sqrt{-i\frac{k_0\rho}{2}\left(\frac{z+d}{\rho}-iA\right)^2}\right]\right\}\cdot\begin{pmatrix}1\\ -\frac{i}{k_0\rho}\end{pmatrix}. \tag{49}$$

Similarly, the rest several integrals can also be evaluated. We write

$$\begin{matrix}G_{\rho_2}\\ G_{\varphi_2}\end{matrix} = i\pi\sum_j \frac{\frac{\gamma_2^*}{k_2^2}-\frac{i\gamma_L^*}{k_T^2}\tan\gamma_L^* l}{q'(\lambda_{jE}^*)}e^{i\gamma_0^*(z+d)}\lambda_{jE}^*\cdot\left[H_0^{(1)}\left(\lambda_{jE}^*\rho\right)\pm H_2^{(1)}\left(\lambda_{jE}^*\rho\right)\right]$$
$$-2k_0^2 A\sqrt{\frac{1}{\pi k_0\rho}}e^{ik_0r_2}\cdot\left\{\sqrt{\frac{\pi}{k_0\rho}}+\frac{\pi}{\sqrt{2}}e^{i\frac{\pi}{4}}A\exp\left[-i\frac{k_0\rho}{2}\left(\frac{z+d}{\rho}-iA\right)^2\right]\right.$$
$$\left.\cdot erfc\left[\sqrt{-i\frac{k_0\rho}{2}\left(\frac{z+d}{\rho}-iA\right)^2}\right]\right\}\cdot\begin{pmatrix}-\frac{i}{k_0\rho}\\ 1\end{pmatrix} \tag{50}$$

and

$$F_{z1} = 2i\pi\sum_j \frac{\frac{\gamma_2^*}{k_2^2}-\frac{i\gamma_L^*}{k_T^2}\tan\gamma_L^* l}{q'\left(\lambda_{jE}^*\right)}e^{i\gamma_{0E}^*(z+d)}\lambda_{jE}^{*2}\cdot H_1^{(1)}\left(\lambda_{jE}^*\rho\right)$$
$$+2ik_0^3 A\sqrt{\frac{1}{\pi k_0\rho}}e^{ik_0r_2}\cdot\left\{\sqrt{\frac{\pi}{k_0\rho}}+\frac{\pi}{\sqrt{2}}e^{i\frac{\pi}{4}}A\exp\left[-i\frac{k_0\rho}{2}\left(\frac{z+d}{\rho}-iA\right)^2\right]\right.$$
$$\left.\cdot erfc\left[\sqrt{-i\frac{k_0\rho}{2}\left(\frac{z+d}{\rho}-iA\right)^2}\right]\right\}. \tag{51}$$

2.3. Evaluation for the Terms of the Magnetic-type (TE) Field

The integrals for the magnetic-type field can be treated in the similar manner to those of the electric-type field. The integral (27) can be rewritten as follows:

$$\begin{matrix}F_{\rho_3}\\ F_{\varphi_3}\end{matrix} = \frac{1}{2}\int_{-\infty}^{\infty}\frac{k_0^2\left(\frac{\gamma_T}{\gamma_2}-i\tan\gamma_T l\right)}{\gamma_T+\frac{\gamma_0\gamma_T}{\gamma_2}-i\left(\gamma_0+\frac{\gamma_T^2}{\gamma_2}\right)\tan\gamma_T l}e^{i\gamma_0(z+d)}$$

$$\cdot[H_0^{(1)}(\lambda\rho) \pm H_2^{(1)}(\lambda\rho)]\lambda d\lambda. \tag{52}$$

The configuration of the poles and the branch cuts are shown in Fig. 3. The pole equation for the integrals (52) is as follows:

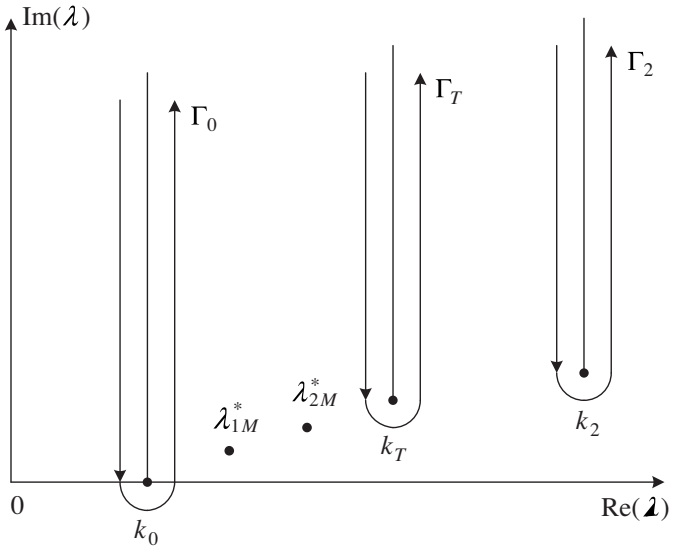

Figure 3. The configuration of the poles and the branch cuts for the magnetic-type (TE) field.

$$p(\lambda) = \gamma_T + \frac{\gamma_0\gamma_T}{\gamma_2} - i\left(\gamma_0 + \frac{\gamma_T^2}{\gamma_2}\right)\tan\gamma_T l \;=\; 0. \tag{53}$$

Next, considering the value $s = k_0/k_2$, the above equation can be rewritten in the following form.

$$p(\lambda, s) = \gamma_T + \frac{s\gamma_0\gamma_T}{k_0\sqrt{1-\lambda^2 s^2/k_0^2}} - i\left(\gamma_0 + \frac{s\gamma_T^2}{k_0\sqrt{1-\lambda^2 s^2/k_0^2}}\right)\tan\gamma_T l = 0. \tag{54}$$

Then, we have

$$\begin{matrix} F_{\rho_3} \\ F_{\varphi_3} \end{matrix} \;=\; i\pi\sum_j \frac{k_0^2\left(\dfrac{\gamma_T^*}{\gamma_2^*} - i\tan\gamma_T^* l\right)}{p'(\lambda_{jM}^*)} e^{i\gamma_{0M}^*(z+d)}\lambda_{jM}^* \cdot\left[H_0^{(1)}(\lambda_{jM}^*\rho) \pm H_2^{(1)}(\lambda_{jM}^*\rho)\right]$$

$$+\frac{1}{2}\int_{\Gamma_0+\Gamma_L+\Gamma_2}\frac{k_0^2\left(\dfrac{\gamma_T}{\gamma_2}-i\tan\gamma_T l\right)e^{i\gamma_0(z+d)}}{p(\lambda)} \cdot\left[H_0^{(1)}(\lambda\rho)\pm H_2^{(1)}(\lambda\rho)\right]\cdot\lambda d\lambda \tag{55}$$

where

$$p'(\lambda_{jM}^*) = -\frac{\lambda_{jM}^*}{\gamma_T^*}-\frac{\lambda_{jM}^*}{\gamma_2^*}\left(\frac{\gamma_T^*}{\gamma_2^*}+\frac{\gamma_0^*}{\gamma_T^*}-\frac{\gamma_0^*\gamma_T^*}{\gamma_2^{*2}}\right)+i\lambda_{jM}^* tan\gamma_T^* l \cdot\left(\frac{1}{\gamma_0^*}+\frac{2}{\gamma_2^*}-\frac{\gamma_T^{*2}}{\gamma_2^{*3}}\right)+\frac{\lambda_{jM}^*}{\gamma_T^*}l\sec^2\gamma_T^* l\left(\gamma_0^*+\frac{\gamma_T^{*2}}{\gamma_2^*}\right). \tag{56}$$

Through analyzing the pole equation, it is found that the following characteristics: When the thickness l satisfied $(k_L^2-k_0^2)^{1/2}\cdot l<\frac{\pi}{2}$, the magnetic-type trapped surface wave cannot be excited. When the thickness of the uniaxial layer increases and satisfies the condition $\frac{\pi}{2}<(k_T^2-k_0^2)^{1/2}\cdot l<\pi$, the magnetic-type trapped surface wave can be excited efficiently. When the thickness l satisfies $(n-\frac{1}{2})\pi<(k_T^2-k_0^2)^{1/2}\cdot l<(n+\frac{1}{2})\pi$, there are n modes of magnetic-type trapped waves.

Similar to the case of electric-type field addressed in Section 2.2, the integration along the branch line Γ_L is zero and the integration along the branch cut Γ_2 can be neglected. So that the next task is to evaluate the integral along the branch cuts Γ_0. Along the researching line for the electric-type case addressed in Section 2.2, we obtain readily.

$$\begin{aligned} I_2 &= \frac{1}{2}\int_{\Gamma_0}\frac{k_0^2\left(\dfrac{\gamma_T}{\gamma_2}-i\tan\gamma_T l\right)}{\gamma_T+\dfrac{\gamma_0\gamma_T}{\gamma_2}-i\left(\gamma_0+\dfrac{\gamma_T^2}{\gamma_2}\right)\tan\gamma_T l}e^{i\gamma_0(z+d)} \cdot\left[H_0^{(1)}(\lambda\rho)\pm H_2^{(1)}(\lambda\rho)\right]\cdot\lambda d\lambda \\ &= -2ik_0^3\sqrt{\frac{1}{\pi k_0\rho}}e^{ik_0 r_2}\left\{\sqrt{\frac{\pi}{k_0\rho}}-\frac{\pi}{\sqrt{2}}e^{i\frac{\pi}{4}}B\exp\left[-i\frac{k_0\rho}{2}\left(\frac{z+d}{\rho}+iB\right)^2\right]\right. \\ &\quad\left.\cdot erfc\left[\sqrt{-i\frac{k_0\rho}{2}\left(\frac{z+d}{\rho}+iB\right)^2}\right]\right\}\begin{pmatrix}-\dfrac{i}{k_0\rho}\\ 1\end{pmatrix} \end{aligned} \tag{57}$$

where

$$B = \frac{\gamma_T - i\dfrac{\gamma_T^2}{\gamma_2}\tan\gamma_T l}{k_0\left(\tan\gamma_T l + i\dfrac{\gamma_T}{\gamma_2}\right)}. \tag{58}$$

And similar approximates have been made by

$$\gamma_0 \approx \sqrt{2}k_0 e^{i\frac{3\pi}{4}}\tau \tag{59}$$

$$\gamma_T \approx \gamma_T' = \sqrt{k_T^2 - k_0^2} \tag{60}$$

$$\gamma_2 \approx \gamma_2' = \sqrt{k_2^2 - k_0^2}. \tag{61}$$

Then, the evaluation of (52) can be obtained as follows:

$$\begin{aligned}\begin{matrix}F_{\rho 3}\\F_{\varphi 3}\end{matrix} &= i\pi\sum_j \frac{k_0^2\left(\dfrac{\gamma_T^*}{\gamma_2^*} - i\tan\gamma_T^* l\right)}{p'(\lambda_{jM}^*)} e^{i\gamma_{0M}^*(z+d)}\lambda_{jM}^* \\ &\quad\cdot\left[H_0^{(1)}\left(\lambda_{jM}^*\rho\right) \pm H_2^{(1)}\left(\lambda_{jM}^*\rho\right)\right] \\ &\quad -2ik_0^3\sqrt{\frac{1}{\pi k_0\rho}}e^{ik_0 r_2}\left\{\sqrt{\frac{\pi}{k_0\rho}} - \frac{\pi}{\sqrt{2}}e^{i\frac{\pi}{4}}B\exp\left[-i\frac{k_0\rho}{2}\left(\frac{z+d}{\rho}+iB\right)^2\right]\right. \\ &\quad \left.\cdot erfc\left[\sqrt{-i\frac{k_0\rho}{2}\left(\frac{z+d}{\rho}+iB\right)^2}\right]\right\}\begin{pmatrix}-\dfrac{i}{k_0\rho}\\1\end{pmatrix}.\end{aligned} \tag{62}$$

Similarly, we get

$$\begin{aligned}\begin{matrix}G_{\rho 3}\\G_{\varphi 3}\end{matrix} &= i\pi\sum_j \frac{\gamma_0^*\left(\dfrac{\gamma_T^*}{\gamma_2^*} - i\tan\gamma_T^* l\right)}{p'(\lambda_{jM}^*)} e^{i\gamma_{0M}^*(z+d)}\lambda_{jM}^* \\ &\quad\cdot\left[H_0^{(1)}(\lambda_{jM}^*\rho) \mp H_2^{(1)}(\lambda_{jM}^*\rho)\right] \\ &\quad +2k_0^2 e^{i\frac{\pi}{4}}\sqrt{\frac{2}{\pi k_0\rho}}e^{ik_0 r_2}\left\{ - e^{i\frac{\pi}{4}}\left(\frac{z+d}{\rho} - iB\right)\sqrt{\frac{\pi}{2k_0\rho}}\right. \\ &\quad\quad +\frac{\pi}{2}B^2\exp\left[-i\frac{k_0\rho}{2}\left(\frac{z+d}{\rho}+iB\right)^2\right] \\ &\quad \left.\cdot erfc\left[\sqrt{-i\frac{k_0\rho}{2}\left(\frac{z+d}{\rho}+iB\right)^2}\right]\right\}\begin{pmatrix}1\\-\dfrac{i}{k_0\rho}\end{pmatrix}\end{aligned} \tag{63}$$

and

$$G_{z1} = 2i\pi \sum_j \frac{\frac{\gamma_T^*}{\gamma_2^*} - i\tan\gamma_T^* l}{p'(\lambda_{jM}^{*2})} e^{i\gamma_{0M}^*(z+d)} \lambda_{jM}^{*2} \cdot H_1^{(1)}(\lambda_{jM}^* \rho)$$
$$-2k_0^2 \sqrt{\frac{1}{\pi k_0 \rho}} e^{ik_0 r_2} \left\{ \sqrt{\frac{\pi}{k_0\rho}} - \frac{\pi}{\sqrt{2}} e^{i\frac{\pi}{4}} B \exp\left[-i\frac{k_0\rho}{2} \left(\frac{z+d}{\rho} + iB \right)^2 \right] \right.$$
$$\left. \cdot erfc\left[\sqrt{-i\frac{k_0\rho}{2}\left(\frac{z+d}{\rho} + iB \right)^2} \right] \right\}. \quad (64)$$

Similar to the case of the electric-type field, the magnetic-type trapped surface wave decreases exponentially by $e^{\sqrt{\lambda_{jM}^{*2} - k_0^2}(z+d)}$ in the $\hat{z}$ direction and attenuates as $\rho^{-\frac{1}{2}}$ in the $\hat{\rho}$ direction, and the magnetic-type lateral wave is contributed from the integration along the branch line Γ_0 and the wave number is k_0.

2.4. The Final Formulations for the Six Field Components

From the above derivations and analysis, and combined with the results for the direct and ideally reflected fields addressed in [1] and [2], the final formulas for the six field components are written readily.

$$E_{0\rho}(\rho,\varphi,z) = -\frac{\omega\mu_0 Idl}{4\pi k_0^2}\cos\varphi \left\{ -\left[\frac{2k_0}{r_1^2} + \frac{2i}{r_1^3} + \left(\frac{z-d}{r_1} \right)^2 \left(\frac{ik_0^2}{r_1} - \frac{3k_0}{r_1^2} - \frac{3i}{r_1^3} \right) \right] \right.$$
$$\cdot e^{ik_0 r_1} + \left[\frac{2k_0}{r_2^2} + \frac{2i}{r_2^3} + \left(\frac{z+d}{r_2} \right)^2 \left(\frac{ik_0^2}{r_2} - \frac{3k_0}{r_2^2} - \frac{3i}{r_2^3} \right) \right] e^{ik_0 r_2}$$
$$\left. + F_{\rho 2} + F_{\rho 3} \right\} \quad (65)$$

$$E_{0\varphi}(\rho,\varphi,z) = \frac{\omega\mu_0 Idl}{4\pi k_0^2}\sin\varphi \left[-\left(\frac{ik_0^2}{r_1} - \frac{k_0}{r_1^2} - \frac{i}{r_1^3} \right) e^{ik_0 r_1} \right.$$
$$\left. + \left(\frac{ik_0^2}{r_2} - \frac{k_0}{r_2^2} - \frac{i}{r_2^3} \right) e^{ik_0 r_2} + F_{\varphi 2} + F_{\varphi 3} \right] \quad (66)$$

$$E_{0z}(\rho,\varphi,z) = \frac{i\omega\mu_0 Idl}{4\pi k_0^2}\cos\varphi \left[-\left(\frac{\rho}{r_1} \right)\left(\frac{z-d}{r_1} \right)\left(\frac{k_0^2}{r_1} + \frac{3ik_0}{r_1^2} - \frac{3}{r_1^3} \right) e^{ik_0 r_1} \right.$$
$$\left. + \left(\frac{\rho}{r_2} \right)\left(\frac{z+d}{r_2} \right)\left(\frac{k_0^2}{r_2} + \frac{3ik_0}{r_2^2} - \frac{3}{r_2^3} \right) e^{ik_0 r_2} + F_{z1} \right] \quad (67)$$

$$B_{0\rho}(\rho,\varphi,z) = -\frac{\mu_0 Idl}{4\pi}\sin\varphi\left[\left(\frac{z-d}{r_1}\right)\left(\frac{ik_0}{r_1}-\frac{1}{r_1^2}\right)e^{ik_0r_1} - \left(\frac{z+d}{r_2}\right)\left(\frac{ik_0}{r_2}-\frac{1}{r_2^2}\right)e^{ik_0r_2} - G_{\rho 2} - G_{\rho 3}\right] \quad (68)$$

$$B_{0\varphi}(\rho,\varphi,z) = -\frac{\mu_0 Idl}{4\pi}\cos\varphi\left[\left(\frac{z-d}{r_1}\right)\left(\frac{ik_0}{r_1}-\frac{1}{r_1^2}\right)e^{ik_0r_1} - \left(\frac{z+d}{r_2}\right)\left(\frac{ik_0}{r_2}-\frac{1}{r_2^2}\right)e^{ik_0r_2} - G_{\varphi 2} - G_{\varphi 3}\right] \quad (69)$$

$$B_{0z}(\rho,\varphi,z) = \frac{i\mu_0 Idl}{4\pi}\sin\varphi\left[-\left(\frac{\rho}{r_1}\right)\left(\frac{k_0}{r_1}+\frac{i}{r_1^2}\right)e^{ik_0r_1} + \left(\frac{\rho}{r_2}\right)\left(\frac{ik_0}{r_2}-\frac{1}{r_2^2}\right)e^{ik_0r_2} + G_{z1}\right] \quad (70)$$

where $r_1 = \sqrt{\rho^2+(z-d)^2}$ and $r_2 = \sqrt{\rho^2+(z+d)^2}$. If Region 2 is made to a perfect conductor by setting $k_2 \longrightarrow \infty$, the above results reduce to the results for the appropriate perfect conductor case addressed in [10].

3. COMPUTATIONS AND CONCLUSIONS

The electromagnetic field of a horizontal electric dipole near the a planar dielectric coated with a uniaxially anisotropic layer includes the direct field, the ideal reflected field, the lateral-wave field, and the trapped surface wave field. Both the terms of lateral wave and those of trapped surface wave can be divided into the electric-type and magnetic-type terms. The total field, the lateral-wave term and trapped-surface-wave terms for the radical electric field components $E_{0\rho}(\rho,0,z)$ and $E_{0\varphi}(\rho,\pi/2,z)$ are computed in several cases and shown in Figs. 4–11, respectively.

From the above analysis and computations, it is concluded as follows: i. The wave numbers of electric-type trapped surface wave, which are between k_0 and k_L, are determined by the operating frequency, the permittivities ε_T and ε_L, and the thickness of the uniaxial layer. Similarly, the wave numbers of the magnetic-type trapped surface wave, which are between k_0 and k_T, are determined by the operating frequency, the permittivity ε_T, and the thickness of the uniaxially anisotropic layer. In the $\hat{z}$ direction, the trapped surface waves of electric type and magnetic type attenuate exponentially

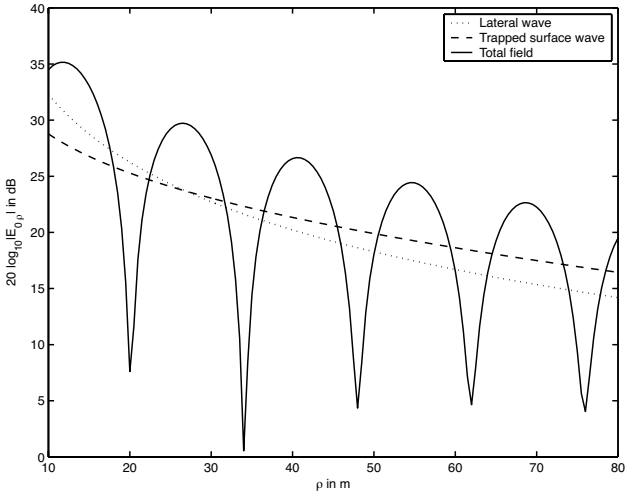

Figure 4. Electric field $|E_{0\rho}(\rho, 0, z)|$ and all terms in V/m with $f = 100\,\mathrm{MHz}$, $\varepsilon_T = 6.25 + 0.02i$, $\varepsilon_L = 4.0 + 0.01i$, $\sqrt{k_T^2 - k_0^2} \cdot l = 0.4\pi$, $\varepsilon_2 = 80$, $\sigma_2 = 4$, $z = d = 0$ m, and $\varphi = 0$.

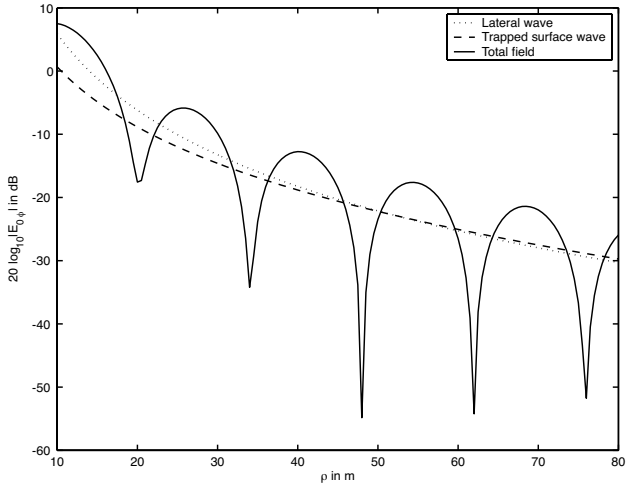

Figure 5. Electric field $|E_{0\varphi}(\rho, \pi/2, z)|$ and all terms in V/m with $f = 100\,\mathrm{MHz}$, $\varepsilon_T = 6.25 + 0.02i$, $\varepsilon_L = 4.0 + 0.01i$, $\sqrt{k_T^2 - k_0^2} \cdot l = 0.4\pi$, $\varepsilon_2 = 80$, $\sigma_2 = 4$, $z = d = 0$ m, and $\varphi = \pi/2$.

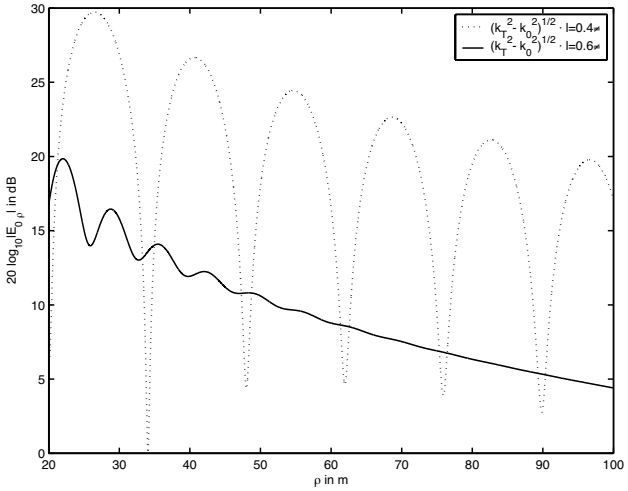

Figure 6. Electric fields $|E_{0\rho}(\rho, 0, z)|$ with $f = 100\,\mathrm{MHz}$, $\varepsilon_T = 6.25 + 0.02i$, $\varepsilon_L = 4.0 + 0.01i$, $\varepsilon_2 = 80$, $\sigma_2 = 4$, $z = d = 0$ m, and $\varphi = 0$ for two different cases: $\sqrt{k_T^2 - k_0^2} \cdot l = 0.4\pi$ and $\sqrt{k_T^2 - k_0^2} \cdot l = 0.6\pi$.

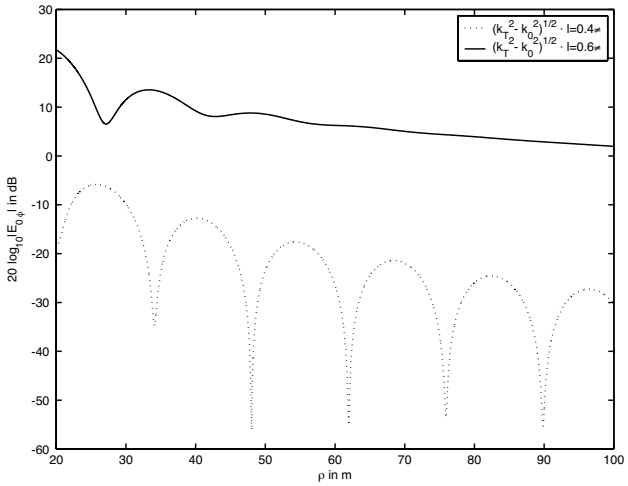

Figure 7. Electric field $|E_{0\varphi}(\rho, \pi/2, z)|$ with $f = 100\,\mathrm{MHz}$, $\varepsilon_T = 6.25 + 0.02i$, $\varepsilon_L = 4.0 + 0.01i$, $\varepsilon_2 = 80$, $\sigma_2 = 4$, $z = d = 0$ m, and $\varphi = \pi/2$ for two different cases: $\sqrt{k_T^2 - k_0^2} \cdot l = 0.4\pi$ and $\sqrt{k_T^2 - k_0^2} \cdot l = 0.6\pi$.

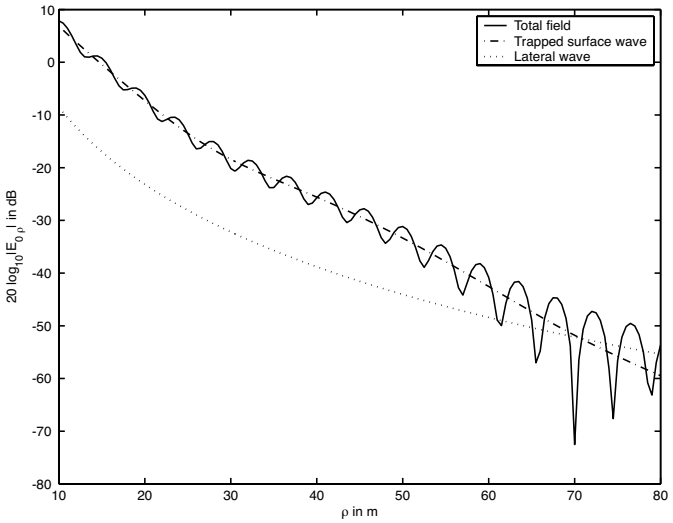

Figure 8. Electric field $|E_{0\rho}(\rho, 0, z)|$ and all terms in V/m with $f = 100\,\mathrm{MHz}$, $\varepsilon_T = 6.25 + 0.02i$, $\varepsilon_L = 4.0 + 0.01i$, $\sqrt{k_T^2 - k_0^2} \cdot l = 0.8\pi$, $\varepsilon_2 = 80$, $\sigma_2 = 4$, $z = d = 0$ m, and $\varphi = 0$.

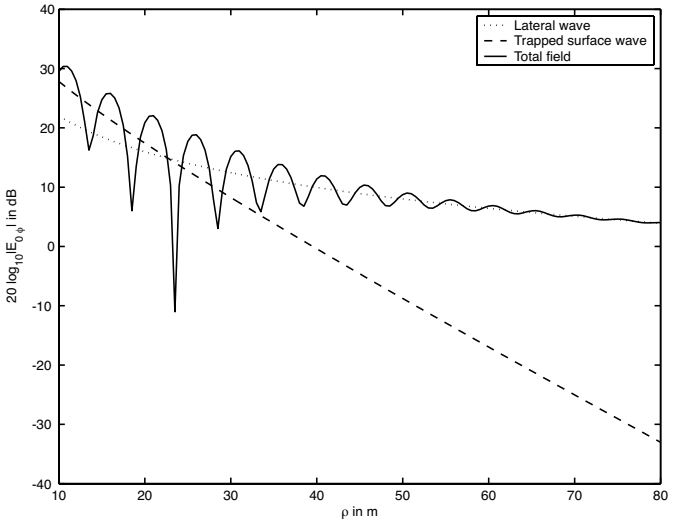

Figure 9. Electric field $|E_{0\varphi}(\rho, \pi/2, z)|$ and all terms in V/m with $f = 100\,\mathrm{MHz}$, $\varepsilon_T = 6.25 + 0.02i$, $\varepsilon_L = 4.0 + 0.01i$, $\sqrt{k_T^2 - k_0^2} \cdot l = 0.8\pi$, $\varepsilon_2 = 80$, $\sigma_2 = 4$, $z = d = 0$ m, and $\varphi = \pi/2$.

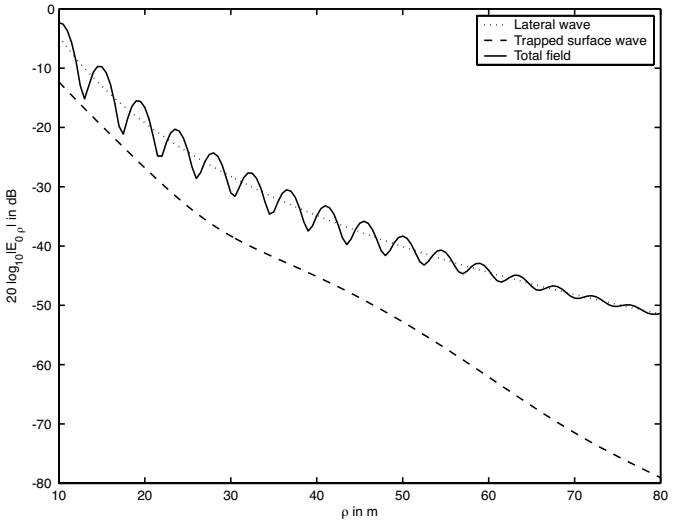

Figure 10. Electric field $|E_{0\rho}(\rho, 0, z)|$ and all terms in V/m with $f = 100\,\text{MHz}$, $\varepsilon_T = 6.25 + 0.02i$, $\varepsilon_L = 4.0 + 0.01i$, $\sqrt{k_T^2 - k_0^2} \cdot l = 0.8\pi$, $\varepsilon_2 = 80$, $\sigma_2 = 4$, $z + d = 0.8$ m, and $\varphi = 0$.

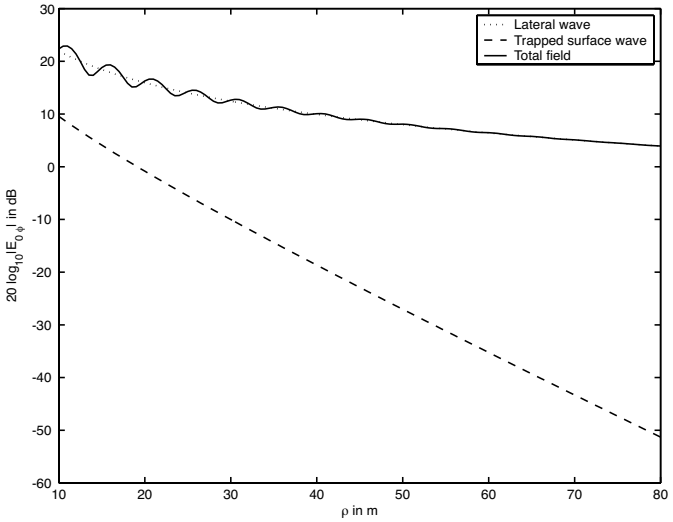

Figure 11. Electric field $|E_{0\varphi}(\rho, \pi/2, z)|$ and all terms in V/m with $f = 100\,\text{MHz}$, $\varepsilon_T = 6.25 + 0.02i$, $\varepsilon_L = 4.0 + 0.01i$, $\sqrt{k_T^2 - k_0^2} \cdot l = 0.8\pi$, $\varepsilon_2 = 80$, $\sigma_2 = 4$, $z + d = 0.8$ m, and $\varphi = \pi/2$.

as $e^{\sqrt{\lambda_{jE}^{*2}-k_0^2}(z+d)}$ and $e^{\sqrt{\lambda_{jM}^{*2}-k_0^2}(z+d)}$, respectively. Therefore, the trapped surface wave can be omitted when the source point or observation point moves away and is not too close to the surface.

ii. It is noted that both the lateral waves of electric type and magnetic type with the wave numbers being k_0 can be excited efficiently.

iii. When the thickness l satisfied $(k_L^2 - k_0^2)^{1/2} \cdot l < \frac{\pi}{2}$, the electric-type trapped surface wave can be excited efficiently and the magnetic-type trapped surface wave cannot be excited. When the thickness of the uniaxial layer increases and satisfies the condition $\frac{\pi}{2} < (k_T^2 - k_0^2)^{1/2} \cdot l < \pi$, the magnetic-type trapped surface wave can be excited efficiently. When the thickness l of the uniaxial layer satisfies $n\pi < \frac{k_T}{k_L}(k_L^2 - k_0^2)^{1/2} \cdot l < (n+1)\pi$, there are $n+1$ modes of the electric-type trapped surface waves. When the thickness l satisfies $(n-\frac{1}{2})\pi < (k_T^2-k_0^2)^{1/2} \cdot l < (n+\frac{1}{2})\pi$, there are n modes of magnetic-type trapped waves. Obviously, in the cases of the thick uniaxial layer, the variation of the total field will be more complex and the interferences occurs for the total field.

iv. Comparing with the results addressed in [10], it is seen that the trapped surface wave for Region 2 being a high lossy dielectric attenuates faster than that for Region 2 being a perfect conductor.

REFERENCES

1. King, R. W. P., M. Owens, and T. T. Wu, *Lateral Electromagnetic Waves: Theory and Applications to Communications, Geophysical Exploration, and Remoting Sensing*, Springer-Verlag, 1992.
2. King, R. W. P., "The electromagnetic field of a horizontal electric dipole in the presence of a three-layered region," *Journal of Applied Phys.*, Vol. 69, No. 12, 7987–7995, 1991.
3. King, R. W. P., "The electromagnetic field of a horizontal electric dipole in the presence of a three-layered region: supplement," *Journal of Applied Phys.*, Vol. 74, No. 8, 4845–4548, 1993.
4. King, R. W. P. and S. S. Sandler, "The electromagnetic field of a vertical electric dipole in the presence of a three-layered region," *Radio Sci.*, Vol. 29, No. 1, 97–113, 1994.
5. Wait, J. R., "Comment on 'The electromagnetic field of a vertical electric dipole in the presence of a three-layered region' by Ronold, W. P. King and Sheldon S. Sandler," *Radio Sci.*, Vol. 33, No. 2, 251–253, 1998.

6. King, R. W. P. and S. S. Sandler, "Reply," *Radio Sci.*, Vol. 33, No. 2, 255–256, 1998.
7. Zhang, H. Q. and W. Y. Pan, "Electromagnetic field of a vertical electric dipole on a perfect conductor coated with a dielectric layer," *Radio Science*, Vol. 37, No. 4, 13-1–13-7, 2002.
8. Zhang, H. Q., K. Li, and W. Y. Pan, "The electromagnetic field of a vertical dipole on the dielectric-coated imperfect conductor," *J. Electromagn. Wavws and Appl.*, Vol. 18, 1305–1320, 2004.
9. Zhang, H. Q., *et al.*, "Electromagnetic field for a horizontal electric dipole buried inside a dielectric layer coated high lossy half space," *Progress In Electromagnetics Research*, PIER 50, 163–186, 2005.
10. Li, K. and Y. Lu, "Electromagnetic field generated by a horizontal electric dipole near the surface of a planar perfect conductor coated with a uniaxial layer," *IEEE Trans. Antennas and Propagat.*, Vol. 53, 3191–3200, 2005.
11. Pan, W. Y., "Surface-wave propagation along the boundary between sea water and one-dimensionally anisotropic rock," *J. Appl. Phys.*, Vol. 58, 3963–3974, 1985.
12. Gradshteyn, I. S. and I. M. Ryzhik, *Table of Integrals, Series, and Products*, Academic Press, New York, 1980.